Percolation between vacancies in the two-dimensional Blume-Capel model

Youjin Deng,[1,2] Wenan Guo,[3] and Henk W. J. Blöte[2,4]
[1]*Laboratory for Materials Science, Delft University of Technology, Rotterdamseweg 137, 2628 AL Delft, The Netherlands*
[2]*Faculty of Applied Sciences, Delft University of Technology, P. O. Box 5046, 2600 GA Delft, The Netherlands*
[3]*Department of Physics, Beijing Normal University, 100875, Beijing, People's Republic of China*
[4]*Lorentz Institute, Leiden University, P. O. Box 9506, 2300 RA Leiden, The Netherlands*
(Received 4 March 2005; published 1 July 2005)

Using suitable Monte Carlo methods and finite-size scaling, we investigate the Blume-Capel model on the square lattice. We construct percolation clusters by placing nearest-neighbor bonds between vacancies with a variable bond probability p_b. At the tricritical point, we locate the percolation threshold of these vacancy clusters at $p_{bc}=0.706\,33(6)$. At this point, we determine the fractal dimension of the vacancy clusters as $X_f=0.1308(5)\approx 21/160$, and the exponent governing the renormalization flow in the p_b direction as $y_p=0.426(2)\approx 17/40$. For bond probability $p_b>p_{bc}$, the vacancy clusters maintain strong critical correlations; the fractal dimension is $X_f=0.0750(2)\approx 3/40$ and the leading correction exponent is $y_p=-0.45(2)\approx -19/40$. The above values fit well in the Kac table for the tricritical Ising model. These vacancy clusters have much analogy with those consisting of Ising spins of the same sign, although the associated quantities ρ and magnetization m are energylike and magnetic quantities, respectively. However, along the critical line of the Blume-Capel model, the vacancies are more or less uniformly distributed over the whole lattice. In this case, no critical percolation correlations are observed in the vacancy clusters, at least in the physical region $p_b\leqslant 1$.

DOI: 10.1103/PhysRevE.72.016101 PACS number(s): 05.50.+q, 64.60.Cn, 64.60.Fr, 75.10.Hk

I. INTRODUCTION

In the development of the theory of tricritical phenomena, a spin-1 Ising model known as the Blume-Capel (BC) model has played an important role. This model was introduced by Blume and Capel [1,2], and the reduced Hamiltonian reads

$$\mathcal{H}/k_{\mathrm{B}}T=-K\sum_{\langle ij\rangle}s_is_j+D\sum_k s_k^2 \quad (s_i=\pm 1,0), \tag{1}$$

where the sum $\langle\ \rangle$ is over all nearest-neighbor pairs of lattice sites. The spins assume values ± 1 and 0, and those in state 0 are referred to as vacancies. The abundance of the vacancies is governed by the chemical potential D, which is also termed the crystal field parameter. The phase diagram for Eq. (1) is sketched in Fig. 1. For $D\to-\infty$, the vacancies are excluded, and the model (1) reduces to Onsager's spin-$\frac{1}{2}$ model [3]. The critical coupling $K_c(D)$ is an increasing function of D. For sufficiently large chemical potential, the transition becomes first order and separates the vacancy-dominated phase from the ordered phase dominated by plus (+1) or minus (−1) spins. At the joint point, these three coexisting phases simultaneously become identical, and this point is called [4] the tricritical point, denoted as (K_t,D_t) in Fig. 1.

In two dimensions, the nature of critical singularities of the BC model is now well established. For the special case $D\to-\infty$, the free energy has already been exactly obtained by Onsager [3,5]. The universal thermal and magnetic exponents are $y_t=1$ and $y_h=15/8$, respectively; these values hold for the whole critical line as follows from universality arguments. At the point (K_t,D_t), universality also predicts that the critical exponents are those exact results obtained by Baxter for a hard-square lattice gas [6,7]. These exponents can also be obtained in the context of the Coulomb gas theory [8,9] and of the conformal field theory [10,11].

According to the latter theory, there exist universality classes characterized by an integer $m=2,3,\ldots$. The associated critical exponents are determined by quantities $\Delta_{p,q}$ defined by

$$\Delta_{p,q}=\frac{[p(m+1)-qm]^2-1}{4m(m+1)}. \tag{2}$$

This equation is known as the Kac formula. The critical dimension X_k of the kth observable operator (energy, magnetization, etc.) satisfies $X_k=\Delta_{p_k,q_k}+\Delta_{p_k',q_k'}$. If the observable is rotationally invariant, the above primed and unprimed labels are equal and one can explicitly write $X_k=X_{p_k,q_k}$. For systems with open surfaces, the number $\Delta_{p,q}$ can also correspond [12–15] to critical dimensions of surface operators. We mention that, in two dimensions, the surfaces are just one-dimensional edges. Further, it was argued [16] that the operators in the so-called unitary grid with $0<p<m$ and 0

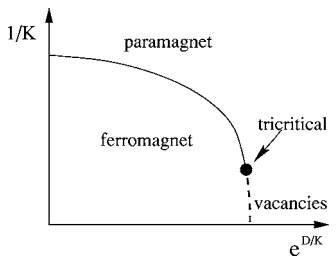

FIG. 1. Sketch of the phase diagram of the BC model. The solid line represents the Ising-like critical line, which separates the para- and ferromagnetic phases; and the first-order transition is shown as a dashed line. The two lines join at a tricritical point (black circle).

TABLE I. The numbers $\Delta_{p,q}$ in the Kac formula for the critical Ising model in two dimensions. The negative values are not shown and are denoted by –. For completeness, the values of p and q are taken in the range $0 \leqslant p,q \leqslant 3$.

	q			
p	0	1	2	3
0	–	1/6	35/48	5/3
1	5/16	0	1/16	1/2
2	21/16	1/2	1/16	0
3	143/28	5/3	35/48	1/6

$< q < m+1$ form a closed operator product algebra, so that critical behavior of physical quantities is described by the numbers in this grid.

The integers $m=3$ and 4 correspond to the critical and the tricritical Ising model in two dimensions, respectively. The thermal and magnetic dimensions of the critical Ising model can be identified as $X_t = X_{2,1}$ and $X_h = X_{2,2}$. The dimension of the second-leading thermal scaling field is $X_{3,1} = 10/3$, which could, in principle, appear in corrections to scaling. However, since $X_{3,1}$ sits outside the closed unitary grid, the number $X_{3,1}$ cannot be observed in thermodynamic quantities. This has been numerically confirmed in Ref. [17]. For the tricritical Ising model ($m=4$), the first-, second-, and third-leading thermal dimensions are identified as $X_{t1} = X_{1,2} = 1/5$, $X_{t2} = X_{1,3} = 6/5$, and $X_{t3} = X_{1,4} = 3$; the last one accounts for corrections to scaling. The magnetic exponents can be interpreted as $y_{h1} = 2 - X_{m/2,m/2} = 77/40$ and $y_{h2} = 2 - X_{m/2,(m-2)/2} = 9/8$ [18]. For later convenience, the numbers generated by the Kac formula (2) are listed in Tables I and II for the critical and the tricritical Ising model, respectively.

Although the numbers outside the closed unitary grid have no thermodynamic analogs, they can still describe critical singularities concerning geometric properties of critical systems. In order to demonstrate this point, we consider the random-cluster representation [19–21] of the Blume-Capel model (1), i.e., percolation clusters are constructed between Ising spins of the same sign by placing nearest-neighbor bonds with probability $p_b^{(\mathrm{KF})} = 1 - \exp(-2K)$. These clusters are known as the Kasteleyn-Fortuin (KF) clusters [19–21].

TABLE II. The number $\Delta_{p,q}$ in the Kac formula for the tricritical Ising model in two dimensions. The negative values are not shown and are denoted by –. For completeness, the values of p and q are taken in the range $0 \leqslant p,q \leqslant 4$.

	q				
p	0	1	2	3	4
0	–	3/16	63/80	143/80	51/16
1	3/10	0	1/10	3/5	3/2
2	99/80	7/16	3/80	3/80	7/16
3	14/5	3/2	3/5	1/10	0
4	399/80	51/16	143/80	63/160	3/16

They have hull-cluster scaling dimensions $X_H(m=3) = X_{0,1} = 1/3$ in Table I and $X_H(m=4) = X_{1,0} = 3/5$ in Table II. These critical KF clusters have the so-called red-bond exponent as $y_p = 2 - X_{0,2} = 13/24$ for the critical Ising model and $y_p = 2 - X_{2,0} = -19/40$ for the tricritical model. This exponent is related to the bond-dilution field and reflects the "compactness" of the critical KF clusters. A remarkable feature is that the bond-dilution field is *irrelevant* for the tricritical Ising model. This means that tricritical KF clusters are so compact that their critical properties are not qualitatively influenced by removing or adding a small fraction of bonds. This has been used to explain the observation that the backbone exponent of the tricritical Ising model is equal to the magnetic exponent [22].

Motivated by the observation that the red-bond exponent satisfies $y_p < 0$ at tricriticality, a number of investigations concerning the geometric properties of the percolation clusters in the Blume-Capel model have been carried out [23,24]. So-called geometric clusters were constructed between Ising spins of the same sign with a variable bond probability $0 \leqslant p_b \leqslant 1$. Thus, for the special case $p_b = 1 - e^{-2K}$, geometric clusters reduce to KF clusters. In addition to the random-cluster fixed point $p_{bc}^{(\mathrm{KF})}$, another fixed point, named the geometric-cluster fixed point, was found for both the critical and the tricritical Ising models [23]. For the critical Ising model, the bond probability at the geometric-cluster fixed point is larger than $p_{bc}^{(\mathrm{KF})}$. From an exact mapping [25], the point can be shown to correspond to the tricritical $q=1$ Potts model. Thus, the fractal dimension is equal to $X_f^{(\mathrm{g})} = X_{m/2,m/2} = X_{3/2,3/2} = 5/96$, and the red-bond exponent at $p_{bc}^{(\mathrm{g})}$ is $y_p = 2 - X_{2,0} = -5/8$ in Table I. Note that $X_{3/2,3/2}$ and $X_{2,0}$ can be interpreted as the magnetic and red-bond scaling dimensions of the tricritical $q=1$ Potts model, respectively. For the tricritical Blume-Capel model on the square lattice, the geometric-cluster fixed point was found at $p_{bc}^{(\mathrm{g})} = 0.6227(2)$, apparently *smaller* than the random-cluster fixed point $p_{bc}^{(\mathrm{KF})} \approx 0.962\,609\,99$. The fractal dimension and the red-bond scaling dimension were determined [23] as $X_f^{(\mathrm{g})} = 0.1311(5)$ and 0.4254(6), which can be identified as $X_{(m+1)/2,(m+1)/2} = X_{5/2.5/2} = 21/160$ and $X_{0,2}$ in the Kac Table II, respectively. The corresponding renormalization flow is sketched in Fig. 2.

In the present work, we address the question: what sort of clustering phenomena exist between vacancies in the two-dimensional Blume-Capel model? In particular, at tricriticality, one may expect to observe critical singularities concerning the geometric distributions of the vacancies, because, in addition to the magnetization, the vacancy density can also be regarded as an independent order parameter.

The organization of the present paper is as follows. Section II briefly reviews the random-cluster representation of the Blume-Capel model, the Monte Carlo algorithms to be used, and the quantities to be sampled. Section III presents simulation results at tricriticality. In Sec. IV we numerically derive the critical Ising line $K = K_c(D)$, and several percolation lines of the vacancy clusters. A brief discussion is given in Sec. V.

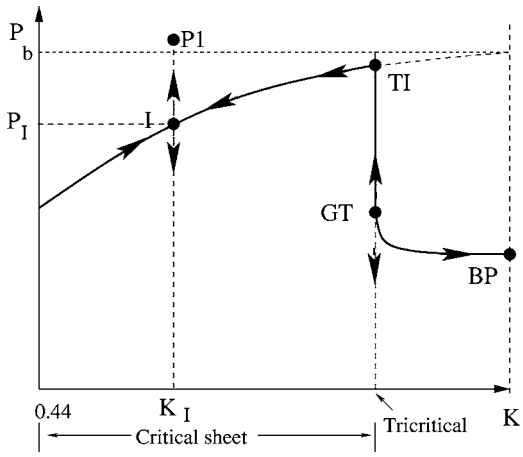

FIG. 2. Renormalization-flow diagram of the Blume-Capel model in the plane of phase transitions parametrized by (K,p_b). The areas $K<K_t$ and $K>K_t$ represent the Ising critical sheet and the region of first-order phase transitions, respectively. The model reduces to the bond percolation model for $K\to\infty$, which has a percolation threshold BP at $p_b=1/2$. We show in total five fixed points, I, P1, TI, GT, and BP, representing the Ising, the tricritical $q=1$ Potts, the tricritical Blume-Capel, the geometric-cluster fixed point of the tricritical Blume-Capel, and the bond percolation models, respectively. Arrows show the directions of the RG flow.

II. MODEL, SIMULATIONS, AND SAMPLED QUANTITIES

The geometric description of fluctuations near a critical point is a subject with a long history. As early as in 1967, Fisher [26] introduced a phenomenological droplet model for the two-dimensional Ising model, in which "geometric clusters" consist of nearest-neighboring (NN) Ising spins of the same sign. These clusters are referred to as Ising clusters, and topological considerations imply [27] that their percolation threshold coincides with the thermal critical point in two dimensions, at least for the square lattice. This statement was further rigorously proved by Coniglio and co-workers [28]. However, it can also be shown [27] that Ising clusters are too dense to correctly describe critical correlations of the Ising model.

Later, Kasteleyn and Fortuin [19,20] showed that the critical properties of the q-state Potts model can indeed be graphically represented by the so-called random-cluster model. The Potts model includes the Ising model as a special case, $q=2$ (for a review, see Ref. [29]), and the reduced Hamiltonian reads

$$\mathcal{H}/k_{\mathrm{B}}T=-K\sum_{\langle ij\rangle}\delta_{\sigma_i\sigma_j}\quad(\sigma=1,2,\ldots,q),\tag{3}$$

where the sum $\langle\ \rangle$ is over all nearest-neighbor pairs, and K is the coupling constant. Then, the random-cluster model can be defined as follows. For each pair of NN spins in the same Potts state, a bond is placed with a probability $p_b^{(\mathrm{KF})}=1-\exp(-K)$, such that the whole lattice is decomposed into groups of sites connected via the occupied bonds. These are just the above KF clusters. The statistical weight of each bond-variable configuration is given by the partition sum of the random-cluster model as

$$Z(u,q)=\sum_b u^{n_b}q^{n_c}\quad(u=e^K-1),\tag{4}$$

where the sum is over all bond-variable configurations, and n_b and n_c are the total numbers of bonds and KF clusters, respectively. Equation (4) is called a Whitney [30] polynomial. Kasteleyn and Fortuin [19,20] showed that the percolation threshold of the KF clusters in Eq. (4) coincides with the transition point of the Potts model (3). Further, scaling properties of KF clusters near criticality are governed by critical exponents of the Potts model (3). For instance, the fractal dimension of KF clusters at criticality is just the magnetic scaling dimension X_h. In fact, one may view the partition sum (4) as a generalization of the Potts model to noninteger q.

The exact mapping between the Potts model (3) and the random-cluster model (4) enabled Swendsen and Wang to develop [31] a cluster Monte Carlo method for the Potts model with integer $q=1,2,\ldots$. This method and its single-cluster version, the Wolff algorithm [32], significantly suppress the critical-slowing-down effect which is very prominent in the standard Metropolis method. Thus, these cluster algorithms have been extensively used in the field of critical phenomena and phase transitions. Recently, a Swendsen-Wang-like cluster algorithm also became available [33,34] to simulate the model (4) with noninteger $q>1$.

Application of the KF mapping to the Blume-Capel model (1) leads to a random-cluster-like partition

$$Z=\sum_{\{v,b\}}u^{n_b}q^{n_c}w^{n_v},\tag{5}$$

where the bonds only occur between nonvacancies. The number of vacancies is denoted as n_v, and the associated weight is $w=e^D$. Since the KF clusters are formed only between Ising spins, no information about the clustering of the vacancies is explicitly contained in Eq. (5).

Owing to the presence of the vacancies in the Blume-Capel model, the Swendsen-Wang or Wolff cluster simulations, which only act on Ising spins, become insufficient. In this case the Metropolis method, which allows fluctuations of the vacancy density, can be used in a combination with these cluster methods. Further, for the special case $D=2\ln 2$, a full-cluster simulation has also been developed [35–37] by mapping the system (1) onto a spin-$\frac{1}{2}$ model with two independent variables $\tau_1=\pm1$ and $\tau_2=\pm1$. Near tricriticality, however, no efficient cluster method is available so far to flip between vacancies and Ising spins. This problem can be partly avoided by means of the so-called geometric-cluster method [38]. This algorithm was developed on the basis of spatial symmetries, such as invariance under spatial inversion and rotation operations. It moves groups of Ising spins and vacancies over the lattice in accordance with the Boltzmann distribution, so that the magnetization and the vacancy density are conserved. In the present work, we used various combinations of the Metropolis, the Wolff, and the geometric-cluster algorithm.

In order to investigate the geometric distributions of the vacancies, we construct percolation clusters between the vacancies with a variable bond probability $0 \leqslant p_b \leqslant 1$, as described in the following. For each pair of nearest-neighbor sites occupied by vacancies, a uniformly distributed random number r is drawn, and a bond is placed if $r < p_b$. As a result, for each configuration, all the vacancies are distributed into a number of connected clusters including single-site clusters. The size of each cluster, defined as the total number of lattice sites in the cluster, is determined and used to calculate the quantities

$$l_2 = \frac{1}{N^2}\left\langle \sum_i n_i^2 \right\rangle \quad \text{and} \quad l_4 = \frac{1}{N^4}\left\langle \sum_i n_i^4 \right\rangle, \tag{6}$$

where the sums are over all the clusters. The parameter n_i is the size of the ith geometric cluster, and $N=L^2$ is the volume of the system. At the percolation threshold, the scaling behavior of these two quantities is governed by an associated exponent that we call, in analogy with KF clusters, the magnetic exponent. The quantity Nl_2 corresponds to the magnetic susceptibility χ in systems undergoing a thermal transition. In percolation theory [39], if the largest cluster is excluded in the sum in Eq. (6), the resulting quantity Nl_2 is known as the mean cluster size, which displays a peak at criticality.

In Monte Carlo studies of phase transitions, certain dimensionless ratios [40] are known to be very helpful, particularly in the determinations of critical points. Thus, on the basis of the quantities defined in Eq. (6), we defined

$$Q = \langle l_2 \rangle^2 / (3\langle l_2^2 \rangle - 2\langle l_4 \rangle). \tag{7}$$

A justification of the above definition of Q can be found in Ref. [41]. At criticality, the asymptotic value of Q is universal; for finite systems, the derivative of Q with respect to the bond probability p_b reflects the associated renormalization exponent in the p_b direction.

III. VACANCY PERCOLATION AT TRICRITICALITY

For simplicity, we chose the Blume-Capel model on the square lattice, of which the tricritical point was located at $K_t=1.64(1), D_t=3.22(2)$ [42]. By means of a sparse transfer matrix technique, the tricritical point has been refined [43] as $K_t=1.643\,175\,9(1), D_t=3.230\,179\,7(2)$, and the vacancy density as $\rho_t=0.454\,950\,6(2)$. The precision is considered to be sufficient for our present investigation.

We simulated the tricritical Blume-Capel model with periodic boundary conditions. Instead of the grand ensemble in the (K,D) plane, we used the canonical ensemble by fixing the total number of vacancies at the tricritical value $L^2\rho_t$, where L is the linear system size. In other words, an external constraint was imposed on the model. We performed simulations of such constrained systems by a combination of the Wolff and the geometric cluster algorithm, as explained above. The scaling behavior of physical quantities at or near the tricritical point has been reported [44,45] for the Blume-Capel model in both two and three dimensions. It was observed [44,45] that the tricritical behavior of energylike quantities is significantly modified by the above constraint, as predicted by the Fisher renormalization mechanism [46]. In particular, the constrained specific heat at tricriticality assumes only a finite value instead of being divergent as $L \to \infty$. Nevertheless, the constraint does not change the universality class and the leading magnetic singularities, and thus our present investigation will not be qualitatively affected by the constraint.

An advantage of the above cluster simulations of constrained systems is that they hardly suffer from critical slowing down, so that the simulation of reasonably large systems requires only modest computer resources. Between subsequent samples, a Swendsen-Wang-like procedure, which decomposes the sites occupied by vacancies into percolation clusters, was performed with bond probability p_b. On this basis, we sampled the size of the largest cluster l_1, the second and the fourth moments of the vacancy-cluster sizes l_2 and l_4, and the dimensionless ratio Q, defined in Sec. II.

We mention that, however, the total number of vacancies at tricriticality $V_t \equiv L^2\rho_t$ is generally not an integer for finite systems, so that the actual simulations took place at $V_- = [V_t] = [\rho_t L^2]$ and $V_+ = [V_t]+1$, where the square brackets [ ] denote the integer part of the number inside. For a sampled quantity A, its tricritical value A_t is obtained by a linear interpolation as $A_t = xA_+ + (1-x)A_-$, with $x = V_t - V_-$; the statistical error margin of A_t is estimated as $\delta A_t = \sqrt{(x\,\delta A_+)^2 + [(1-x)\,\delta A_-]^2}$.

A. Percolation threshold

As mentioned above, the universal ratio Q is very useful in numerical determinations of critical points. When a physical parameter, such as the bond probability p_b, is varied, the occurrence of a critical point is normally accompanied by an intersection between the Q data lines for different system sizes L. More generally, such intersections correspond to fixed points in the context of renormalization group (RG) theory. The fixed points can still be relevant or irrelevant. If it is relevant, the slope of the Q data lines increases with L, and this increase is governed by the scaling exponent associated with the parameter that is varied. As a consequence, the slope at criticality diverges for $L \to \infty$.

We simulated 14 system sizes in the range $8 \leqslant L \leqslant 200$; about 3×10^8 samples were taken for each system size. Each sample was preceded by about $L/5$ Wolff- and $L/3$ geometric-cluster flips. Part of the Q data is shown in Fig. 3. The rather clean intersection implies a percolation threshold near $p_b=0.71$. In order to locate the transition and determine the associated renormalization exponent in the p_b direction, we fitted the Q data according to the least-squares criterion by

$$\begin{aligned} Q(p_b,L) = Q_c &+ \sum_{k=1}^{4} a_k (p_b - p_{bc}^{(g)})^k L^{k y_p} + \sum_{l=1}^{4} b_l L^{y_l} \\ &+ c(p_b - p_{bc}^{(g)}) L^{y_p + y_i} + n(p_b - p_{bc}^{(g)})^2 L^{y_p} + r_0 L^{y_a} \\ &+ r_1 (p_b - p_{bc}^{(g)}) L^{y_a} + r_2 (p_b - p_{bc}^{(g)})^2 L^{y_a} \\ &+ r_3 (p_b - p_{bc}^{(g)})^3 L^{y_a}, \end{aligned} \tag{8}$$

where the terms with amplitude b_l account for various finite-

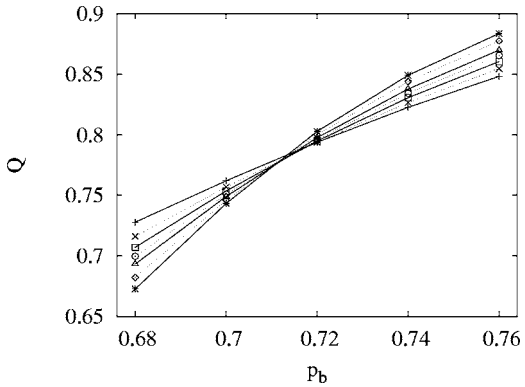

FIG. 3. Dimensionless ratio Q for the two-dimensional BC model at tricriticality vs the bond probability p_b between vacancies. The data points +, ×, □, ◯, △, ◇, and * represent $L=16$, 24, 32, 40, 48, 64, and 80, respectively. The intersections indicate the percolation threshold of the vacancy clusters.

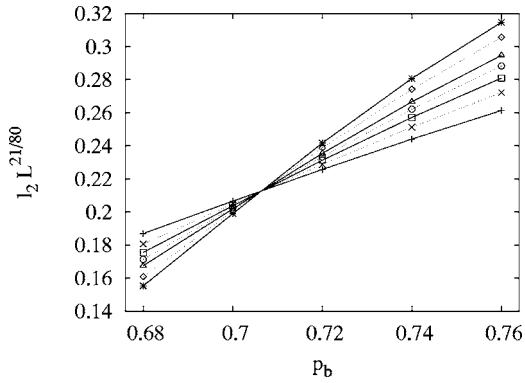

FIG. 4. Second moment of the cluster-size distribution for the two-dimensional BC model at tricriticality, shown as $l_2 L^{21/80}$ vs the bond probability p_b between the vacancies.

size corrections. This equation follows from an expansion of the finite-size scaling formula for Q, as given, e.g., in Ref. [37]. Following the work in Ref. [23], we have used the superscript (g) to denote quantities concerning geometric clusters. Since the leading irrelevant thermal scaling field in the universality class of the tricritical Ising model has an exponent $y_i=-1$, we simply set $y_l=-l$ with $l=1$, 2, 3, and 4. The term with coefficient n reflects the nonlinear dependence of the scaling field on the bond probability p_b, and the one with c describes the mixed effect of the relevant and irrelevant scaling fields. The terms with amplitudes r_0, r_1, r_2, and r_3 arise from the analytic part of the free energy, and the exponent y_a is equal to $2X_f-2$ where X_f is the fractal scaling dimension for the percolation clusters at $p_{bc}^{(g)}$. As will be determined later, the value is $X_f=0.1308(6)\approx 21/160$, so that we fixed the exponent y_a at $-139/80$. From satisfactory fits, as judged from the residual χ^2 compared with the number of degrees of freedom, we obtain $p_{bc}^{(g)}=0.7063(1)$, $Q_c=0.7606(6)$, and $y_p=0.4255(15)$.

We also fitted the data for the second moment of the cluster sizes l_2 by

$$l_2(p_b,L)=L^{-2X_f}\Bigg(a_0+\sum_{k=1}^{4}a_k(p_b-p_{bc}^{(g)})^k L^{ky_p}+\sum_{l=1}^{4}b_l L^{y_l}+c(p_b-p_{bc}^{(g)})L^{y_p+y_i}+n(p_b-p_{bc}^{(g)})^2L^{y_p}+r_0L^{y_a}+r_1(p_b-p_{bc}^{(g)})L^{y_a}+r_2(p_b-p_{bc}^{(g)})^2L^{y_a}+r_3(p_b-p_{bc}^{(g)})^3L^{y_a}\Bigg). \quad (9)$$

We obtain $p_{bc}^{(g)}=0.706\,25(14)$, $a_0=0.2114(3)$, $y_p=0.4232(16)$, and $X_f=0.1308(6)$. The results for the critical point $p_{bc}^{(g)}$ and the exponent y_p are in good agreement with those obtained from the ratio Q. As an illustration, part of the data for l_2 is shown in Fig. 4 as $l_2L^{21/80}$ versus the bond probability p, where a justification for the number 21/80 will be given later. As expected, the quantity $l_2L^{21/80}$, though nonuniversal, also displays a clean intersection near p_c.

B. Bond probability $p_b=1$

Naturally, one can now address the following question. Beyond the critical percolation threshold, i.e., $p_b>p_{bc}^{(g)}$, does the largest cluster also occupy a finite fraction of the whole lattice as for conventional percolation? If not, what is the fractal dimension of the percolation clusters for $p_b>p_{bc}^{(g)}$?

We fixed the bond probability at $p_b=1$ such that the percolation game reduces to correlated site percolation between vacancies. Again, we simulated at the tricritical point with a fixed number of vacancies. The system sizes took 19 numbers in the range $8\leqslant L\leqslant 600$. The numbers of samples per system size are about 6×10^7 for $L\leqslant 160$, 3×10^7 for $160<L\leqslant 240$, and 1.5×10^7 for $L>240$. The data for the ratio Q and the quantity l_2 are shown in Table III. We fitted the Q data by

$$Q(L)=Q_c+b_1L^{y_{vi}}+b_2L^{-1}+b_3L^{-2}+b_4L^{-3}, \quad (10)$$

where the existence of the finite-size exponents -1, -2, and -3 has been explained earlier. In addition, we include a term with an unknown exponent y_{vi}, in which the subscript vi refers to an irrelevant correction in the percolation between vacancies. Satisfactory fits were obtained including system sizes down to $L=12$. We obtain $Q_c=0.9808(1)$, $y_{vi}=0.45(2)\approx -19/40$, and the amplitude $b_1=-0.041(1)$. Despite being close to 1, it is still clear that Q_c is not equal to 1. This indicates that strong critical correlations remain in the percolation clusters between vacancies for $p_b=1$. The fit of Q is illustrated in Fig. 5. The approximate linearity for large L shows that the leading finite-size correction indeed has an exponent near the aforementioned value $y_{vi}=-19/40$.

On the basis of the above fit for Q, we conclude that the asymptotic value of l_2 for $L\to\infty$ vanishes. Accordingly, we fitted the l_2 data by

$$l_2(L)=L^{-2X_f}(b_0+b_1L^{y_{vi}}+b_2L^{-1}+b_3L^{-2}+b_4L^{-3}+r_0L^{2X_f-2}), \quad (11)$$

where the term with amplitude r_0 arises from the analytic part of the free energy, and the exponent was fixed at $-19/40$. We obtain $X_f=0.0750(1)$, which agrees with the magnetic scaling dimension $X_h=3/40$, describing the scaling of the magnetization in the two-dimensional tricritical Ising

TABLE III. Monte Carlo data for the dimensionless ratio Q and the second moment of the cluster size l_2 for the tricritical Blume-Capel model. The bond probability is $p_b=1$.

L	8	10	12	14	16	20
Q	0.97628(2)	0.97464(1)	0.97378(1)	0.97330(1)	0.97304(1)	0.97287(1)
l_2	0.192552(6)	0.188831(5)	0.185634(5)	0.182852(5)	0.180407(4)	0.176228(5)
L	24	28	32	40	48	64
Q	0.97297(1)	0.97312(1)	0.97332(1)	0.97373(1)	0.97412(1)	0.97475(1)
l_2	0.172785(5)	0.169854(4)	0.167296(4)	0.163016(4)	0.159533(4)	0.154049(3)
L	80	120	160	240	360	600
Q	0.97526(1)	0.97610(1)	0.97664(1)	0.97730(1)	0.97790(1)	0.97845(1)
l_2	0.149843(3)	0.142298(3)	0.137067(3)	0.129869(4)	0.122938(4)	0.114573(4)

universality class. Accordingly, we show the data for $l_2 - b_1 L^{y_{vi}-2X_f}$ in Fig. 6 versus $L^{-3/20}$, where the value $b_1 = -0.179(5)$ was taken from the fit.

In short, we show that, in addition to the fluctuations of the vacancy density ρ, the geometric properties of the vacancy clusters at tricriticality also display singular behavior. The tricritical scaling behavior of ρ is governed by the thermal exponents which are $y_{t1}=9/5$ and $y_{t2}=4/5$ for the tricritical Ising model. The question then arises of the exact values of renormalization exponents concerning critical properties of the vacancy clusters. Some insight can be provided by comparing our numerical results with the Kac table (Table II) and with the work in Ref. [23]. For the percolation clusters of Ising spins of the same sign, a percolation threshold at the tricritical point was found [23] at $p_{bc}^{(g)}=0.6227(2)$, smaller than the value $p_{bc}^{(KF)}=1-e^{-2K_t}\approx 0.962\,609$ Ref. [43] at the random-cluster point. At $p_{bc}^{(g)}$, the fractal dimension X_f and the exponent y_p were conjectured [23] to correspond to $X_{(m+1)/2,(m+1)}=X_{5/2,5/2}=21/160$ and $2-X_{0,2}=17/40$. The numbers $X_{5/2,5/2}$ and $X_{0,2}$, respectively, correspond to the magnetic and red-bond scaling dimensions of the *critical* $q=2+2\cos(2\pi/5)$ Potts model, respectively; this model has the same central charge c as the tricritical Ising model. For $p_b > p_{bc}^{(g)}$, the scaling of these Ising-spin clusters is governed by the *irrelevant* random-cluster point $p_{bc}^{(KF)}$, where the red-bond exponent is $y_p=2-X_{2,0}=-19/40$ [23]. From the numerical analyses in the present section, one notes that the percolation clusters of vacancies have close analogy with the above Ising-spin clusters. Although these two types of clusters percolate at different bond probabilities $p_{bc}^{(g)}$, they have the same RG exponents at the thresholds: within the estimated error margins, the fractal dimension is $X_f=21/160$ and the red-bond exponent is $y_p=17/40$. A similar statement also applies to the case $p_b > p_{bc}^{(g)}$: both clusters have fractal dimension $X_f=X_{2,2}=3/40$, and the associated correction-to-scaling exponent is $y_{vi}=-19/40$. These similarities may seem striking, because the vacancy density ρ and the magnetization m are of a different nature: they are energylike and magnetic quantities, respectively.

IV. GENERAL PHASE DIAGRAM

In addition to the tricritical point (K_t, D_t), we are also interested in the general phase transitions in the plane (K, D) or (K, ρ). In particular, we ask the question, to what extent can the Ising critical behavior along the critical Ising line be reflected in the geometric properties of the vacancy clusters. For the chemical potential $D \ll 0$, the Blume-Capel model only contains a small number of vacancies. Thus, it is natural

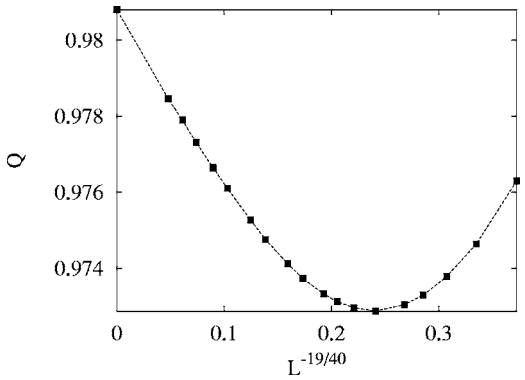

FIG. 5. Finite-size dependence of the dimensionless ratio Q for the two-dimensional BC model at tricriticality for bond probability $p_b=1$ between the vacancies.

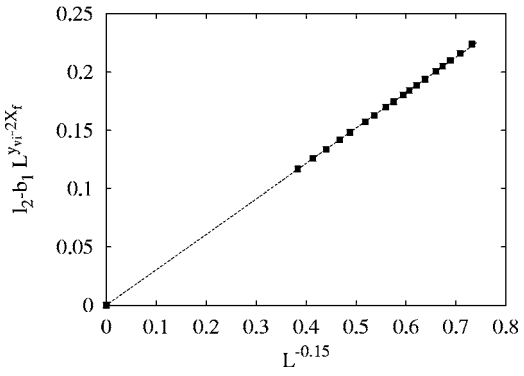

FIG. 6. Second moment of cluster size l_2 for the two-dimensional BC model at tricriticality, vs $L^{-0.15}$. The exponent 0.15 is equal to $2X_f=3/20$, the bond probability is 1, and the exponent y_{vi} is fixed at $-19/40$.

TABLE IV. Fits for the Ising (tri)critical points and the percolation thresholds with bond probability $p_b=1$. The parameter K_2 is equal to $\ln(1+\sqrt{2})/2$ for the Ising critical transition and 0.4 for the percolation. The symbol – means that Ising criticality does not exist for $K=0$.

K	0.0	K_2	0.5	0.6	0.7	0.8	0.9
D(Ising)	–	$-\infty$	−0.99893(8)	0.06954(6)	0.64310(6)	1.0610(1)	1.4037(1)
ρ(Ising)	–	0	0.0756(1)	0.1687(5)	0.2343(5)	0.2825(5)	0.3207(5)
$D(p_b=1)$	1.06848(1)	1.1867(1)	1.2561(1)	1.3434(1)	1.4500(1)	1.5769(1)	1.7244(1)
$\rho(p_b=1)$	0.592746(1)	0.58857(1)	0.58583(1)	0.58208(1)	0.57709(1)	0.57067(1)	0.56247(1)
K	1.0	1.1	1.2	1.3	1.4	1.6431758(1)	
D(Ising)	1.7027178(2)	1.97417(6)	2.2272(1)	2.4668(1)	2.6969(1)	3.2301797(2)	
ρ(Ising)	0.3495830(2)	0.3725(5)	0.3911(5)	0.4082(5)	0.4240(5)	0.4549506(2)	
$D(p_b=1)$	1.8919(1)	2.0770(1)	2.2770(1)			3.2301797(2)	
$\rho(p_b=1)$	0.55246(1)	0.54028(1)	0.52654(2)			0.4549506(2)	

that critical percolation correlations do not occur for $D \ll 0$. A sparse transfer matrix technique was applied [43] to find the critical point at $K=1$ as $D_c=1.702\,717\,8(2)$; the corresponding vacancy density is $\rho_c=0.349\,583\,0(2)$. This critical point is significantly far from the tricritical point (K_t,D_t), and thus crossover phenomena are absent. We have Monte Carlo simulated this critical point and constructed vacancy clusters with bond probability $p_b=1$. Precisely at the critical point $K_c=1$, $D_c=1.702\,717\,8(2)$, we observe that, for $L\to\infty$, the dimensionless ratio $Q(L)$ approaches the Gaussian value 1/3, and the second moment of the cluster sizes l_2 vanishes rapidly. This describes the situation that the vacancy clusters remain finite at the critical point. Similar phenomena were observed for other critical points.

Nevertheless, for the Blume-Capel model with finite couplings K, the vacancy clusters with bond probability $p_b=1$ must percolate if the chemical potential D is sufficiently enhanced—i.e., there are sufficient vacancies on the square lattice. An example is the case $K=0$, where the present percolation problem reduces to the conventional uncorrelated site percolation model for the vacancies. For this case, the site percolation threshold is not exactly known, but has been numerically determined [47,48] with a considerable precision as on the square lattice. In the language of the chemical potential D, one has $D_c(K=0)=1.068\,477\,3(4)$ from the relation $\rho=e^D/(2+e^D)$. The previous paragraph shows that the vacancy clusters with $p_b \leqslant 1$ do not percolate along the Ising critical line. Thus, for the Blume-Capel model with couplings $K<K_t$, one simply expects that the line of percolation thresholds $D_c(K)$ for $p_b=1$ lies in the paramagnetic state.

Section III demonstrates that, at the tricritical point (K_t,D_t), the vacancy clusters exhibit critical percolation correlations for bond probability $p_b>p_{bc}^{(g)}$. In other words, the point (K_t,D_t) is always a percolation threshold of the vacancy percolation problem defined in the parameter plane (K,D) as long as the fixed bond probability $p_b>p_{bc}^{(g)}$. Thus, it is plausible that the tricritical point (K_t,D_t) serves as the joint point of the Ising critical line $K_c(D)$ and the percolation lines $D_c(K)$ for $p_b>p_{bc}^{(g)}$, including the case $p_b=1$. This expectation will be numerically confirmed later.

A. Ising critical line

Along the critical line $K_c(D)$, we determined critical points for 12 uniformly distributed values of the couplings K in the range $0.4 \leqslant K \leqslant 1.5$. The grand ensemble of the Blume-Capel model was simulated by means of a combination of the standard Metropolis sweeps and Wolff-cluster steps. For most values of the above couplings, no severe critical slowing down was observed although it must be present near the tricritical point. The determination of the critical points also used a dimensionless ratio, which is here defined as $Q=\langle m^2\rangle^2/\langle m^4\rangle$. For the two-dimensional universality class, the asymptotic value of the ratio Q for $L\to\infty$ has been determined as $Q_c=0.856\,215\,7(5)$ [49]. From the exact expression of the two- and four-point correlation functions on the basis of conformal field theory, the value of Q_c has also been numerically evaluated [50–52] as $Q_c=0.856\,221(4)$.

The Q data were fitted by Eq. (8), in which the parameters p and y_p are replaced by D and $y_t=1$, respectively. The finite-size-correction exponents were taken as follows. The irrelevant scaling exponent is $y_1=y_i=-2$ in the two-dimensional Ising universality class. The exponent y_2 was set at $y_t-2y_h=-11/4$. Such corrections arise from the nonlinear dependence of the temperature scaling field on the magnetic field. The exponents y_3 and y_4 were simply fixed at −4 and −5, respectively. The terms with y_3 and y_4 were not included in most of the fits of the Q data, because the fits did not give clear evidence for the presence of these terms. The exponent y_a from the analytic contribution is equal to $d-2y_h=-7/4$. During the fits, the value Q_c was fixed at $0.856\,215\,7(5)$, and the results are shown in Table IV.

The vacancy density ρ is an energylike quantity, and its scaling behavior near criticality can be obtained by differentiating the free energy with respect to the thermal field, which leads to

$$\rho(D,L) = v_0 + \sum_{i=1}^{3} v_i (D-D_c)^i + L^{-X_t}\Bigg(a_0 + \sum_{k=1}^{4} a_k (D-D_c)^k L^{k y_t} + b_1 L^{-2} + b_2 L^{-3} + b_3 L^{-4} + c(D-D_c)L^{y_t-2} + n(D-D_c)^2 L^{y_t}\Bigg), \tag{12}$$

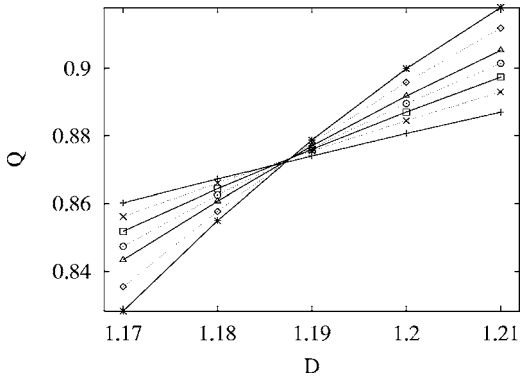

FIG. 7. Dimensionless ratio Q for the disordered BC model vs the chemical potential D. The coupling constant is $K=0.4$, and the bond probability p_b between vacancies is 1. The data points +, ×, □, ◯, △, ◇, and * represent $L=16$, 24, 32, 40, 48, 64, and 80, respectively.

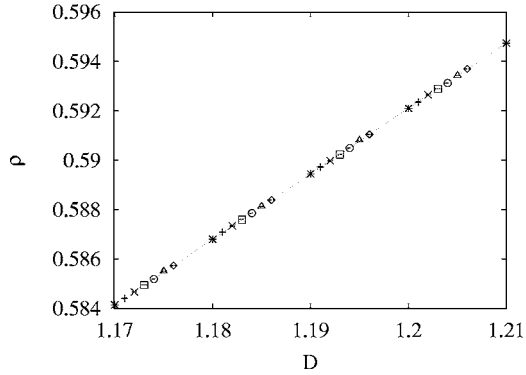

FIG. 8. Vacancy density ρ for the disordered BC model vs the chemical potential D. The coupling constant is $K=0.4$. The data points +, ×, □, ◯, △, ◇, and * represent $L=16$, 24, 32, 40, 48, 64, and 80, respectively. The error bars are much smaller than the size of the data points.

where the terms with v_i (for $i=0,1,2,3$) account for the analytic contributions. The thermal scaling dimension is fixed at $X_t=1$, and the results are also listed in Table IV.

B. Percolation line with $p_b=1$

Except for the tricritical point (K_t,D_t), the percolation threshold for the vacancy clusters with $p_b=1$ occurs in the paramagnetic region of the Blume-Capel model, as discussed above. Thus, it must be in the universality class of conventional percolation in two dimensions, which has thermal and magnetic exponents $y_t=3/4$ and $y_h=91/48$ [39], respectively. The universal ratio Q, defined in Eq. (7), has been determined [41] as $Q_c=0.870\,53(2)$ from the conventional uncorrelated bond percolation model on the square lattice, of which the percolation threshold is exactly known as $p_c=1/2$ [29,39]. An example of the Q data is given in Fig. 7 for the case $K=0.4$. Following the fits for the Ising critical line $D_c(K)$, the data for Q were also fitted by Eq. (8) with $y_p=y_t=3/4$ and $y_a=2-2y_h=-43/24$. The results for $D_c(K)$ were shown in Table IV.

Since the percolation line $D_c(K)$ lies in the paramagnetic region, the vacancy density ρ is an analytic function of the couplings K and the chemical potential D. This is reflected by Fig. 8, where the ρ data for different system sizes almost collapse into a single line. Thus, for each given coupling constant K, we fitted the ρ data by

$$\rho(D,L) = \rho_{sc} + \sum_{i=1}^{4} v_i (D - D_c)^i + b e^{-L/\xi} + c_1 (D - D_c) e^{-L/\xi}. \tag{13}$$

The unknown parameter ξ represents the correlation length between vacancies, which is finite in the paramagnetic region even for $L\to\infty$. Accordingly, the corrections to scaling appear in an exponential form in Eq. (13). Apparently, the fits of $\rho(D,L)$ by Eq. (13) cannot be used to determine the percolation threshold D_c. Thus, the values of D_c were taken from those obtained from the Q data. The results for ρ_c were shown in Table IV, where the error margins have already taken into account the uncertainties of D_c.

C. Percolation lines with $p_b=0.7063$ and $1/2$

We have seen in Sec. II that vacancy clusters with bond probability $p_b=0.7063$ percolate at the tricritical point. In the limit $K=0$ and $D\to\infty$, where the whole square lattice is occupied by the vacancies, the clusters already percolate at $p_b=1/2$. Thus, for $K=0$, the mixed site-bond percolation with $p_b=0.7063$ must also have a transition in the physical region, i.e., $\rho\leqslant 1$. This statement may be expected to hold for a range of nonzero couplings K.

We simulated the Blume-Capel model in the plane (K,D) and constructed vacancy clusters with bond probability $p=0.7063$. The determination of the associated percolation line also makes use of the universal ratio Q defined in Eq.

TABLE V. Fits for the percolation thresholds with bond probability $p_b=0.7063$.

K	0.0	0.4	0.8	1.0	1.2	1.4	1.5
D	1.87756(1)	1.94281(1)	2.14704(1)	2.30973(1)	2.52100(1)	2.79144(1)	2.95418(1)
ρ	0.765639(4)	0.763783(4)	0.756606(4)	0.749621(4)	0.738194(4)	0.716985(4)	0.696493(4)
K	1.52	1.54	1.56	1.58	1.60	1.62	1.6431759(2)
D	2.98943(1)	3.02561(1)	3.06284(1)	3.10120(1)	3.14067(1)	3.18149(1)	3.23017970(4)
ρ	0.690595(4)	0.683713(4)	0.674682(4)	0.665556(4)	0.651930(4)	0.625930(4)	0.4549506(2)

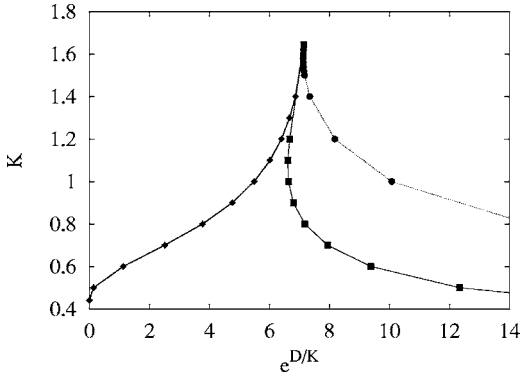

FIG. 9. Thermal and percolation phase diagram of the two-dimensional BC model in the (K,D) plane. The data points $\diamond$, connected by the thick solid line, represent Ising phase transitions between the para- and ferromagnetic states. The symbols $\square$ on the thin solid line represent percolation thresholds for bond probability $p_b=1$. The symbols $\bigcirc$ on the dotted line are for the percolation thresholds for $p_b=0.7073$. All the percolation thresholds with $p_b > 0.7073$ end at the tricritical point (K_t,ρ_t).

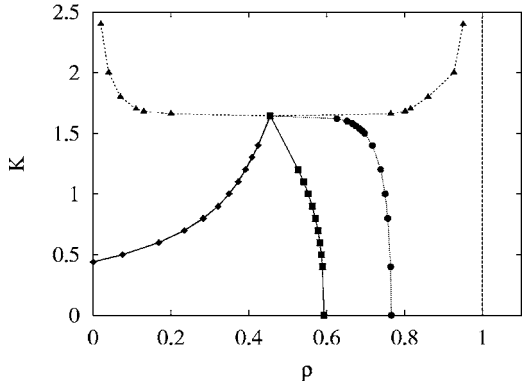

FIG. 10. Thermal and percolation phase diagram of the two-dimensional BC model in the (K,ρ) plane. The data points $\diamond$, connected by the thick solid line, represent Ising phase transitions between the para- and ferromagnetic states. The symbols $\square$ on the thin solid line represent percolation thresholds for bond probability $p=1$. The symbols $\bigcirc$ on the dotted line are for the percolation thresholds for $p_b=0.7073$. The vertical line is for the bond percolation between vacancies with $p_b=1/2$. The first-order transition is represented by the dashed line on which the data points are denoted by $\triangle$. All the percolation thresholds with $1 \geqslant p_b \geqslant 0.7073$ end at the tricritical point (K_t,ρ_t), while those for $1/2 < p_b < 0.7073$ join at the line of first-order transitions.

(7), and the finite-size analysis of the Monte Carlo data follows the same procedure as that for the case $p_b=1$. We skip the description of the detailed fitting procedures, and list the results in Table V.

On the basis of Tables IV and V, we sketch the general phase diagram for the Blume-Capel model in Figs. 9 and 10, which apply to the parameter planes (K,D) and (K,ρ), respectively. It is rather interesting to see that the tricritical point (K_t,D_t) indeed serves as a joint point for the line of Ising critical transitions, the site percolation line $(p_b=1)$, and the percolation line with $p_b=0.7063$. In fact, all the percolation lines with bond probabilities $0.7063 \leqslant p_b \leqslant 1$ will end at the tricritical point. If one were to investigate the percolation model at the unphysical bond probability $p_b>1$ (this is, for instance, possible by means of a transfer-matrix technique), it is very plausible that there exist a range $p_b>1$ for which the percolation lines still end at the tricritical point (K_t,D_t).

For the limit $D_c \to \infty$, the percolation problem between vacancies reduces to the conventional bond percolation problem, and the percolation threshold occurs at bond probability $p_b=1/2$. This holds for all finite couplings K, as shown by the vertical line at vacancy density $\rho=1$ in Fig. 10.

D. Line of first-order transitions

For completeness, we also derive the line of first-order phase transitions of the Blume-Capel model for couplings $K > K_t$. It is shown in Fig. 10. At zero temperature $K \to \infty$, the lattice is fully occupied either by the vacancies, by -1 Ising spins, or by $+1$ spins. This transition occurs at $K_c/D_c=1/2$. For $K_t < K < \infty$, we determined the transition points by means of the cluster-variation method developed by Kikuchi [53–55]. This method is a generalization of the mean-field approximation, and has been extensively applied in calculations of phase diagrams in the field of material science [56,57]. In the mean-field theory, every spin on the lattice interacts equivalently with all other spins. As a result, for the Ising model, the configurational entropy per spin can be simply written as

$$S = -k_B(x_+ \ln x_+ + x_- \ln x_-) = -\frac{1}{2}k_B[(1+m)\ln(1+m) + (1-m)\ln(1-m) - 2\ln 2]. \tag{14}$$

Here, the parameters x_+ and x_- are the densities of the $+1$ and the -1 spins, respectively, and $m=x_+-x_-$ is the magnetization density. In Eq. (14), the entropy contributions from pair

TABLE VI. Results of the first-order phase transitions in the Blume-Capel model, as obtained from the square-cluster approximation of the cluster variation method. The vacancy density at the coexistent can assume two values, as represented by p_1 and p_2.

K	1.66	1.68	1.70	1.80	2.00	2.40	∞
D	3.240	3.290	3.335	3.556	3.960	4.776	∞
D/K	1.952	1.958	1.962	1.975	1.980	1.990	2
ρ_1	0.236	0.132	0.110	0.073	0.044	0.028	0
ρ_2	0.764	0.868	0.890	0.927	0.956	0.972	1

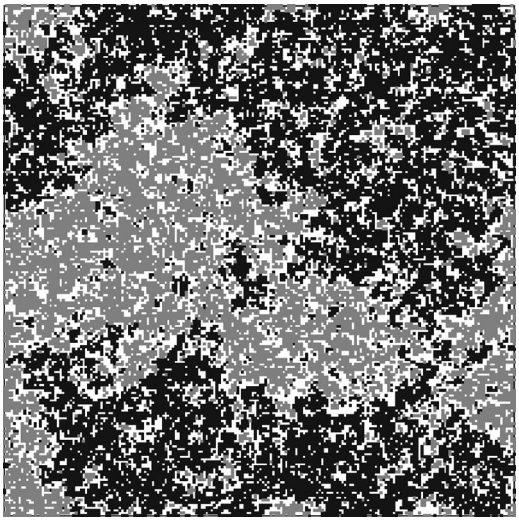

FIG. 11. A typical configuration of the vacancy distribution along the Ising critical line in Fig. 1. The critical point here is $K=1, D=1.702\,717\,8(2)$. The system size is 200×200. The + and − Ising spins are shown as the black and gray points, and the vacancies correspond to the white background. The nonequivalence between + and − Ising spins is due to the finite-size effect.

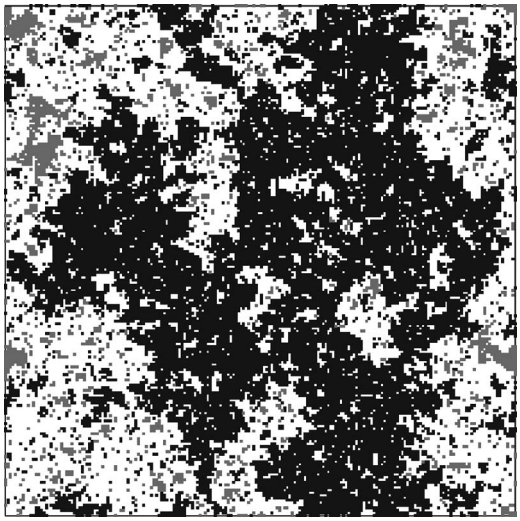

FIG. 12. A typical configuration of the vacancy distribution at the tricritical point (K_t, D_t). The critical point here is $K=1.643\,175\,8(1), D=3.230\,179\,7(2)$. The system size is 200×200. The + and − Ising spins are shown as the black and gray points, and the vacancies correspond to the white background. The nonequivalence between + and − Ising spins is due to the finite-size effect.

and multiple-point correlations are ignored. Naturally, a better approximation of the entropy S can be achieved by taking into consideration a cluster consisting of n spins. If the cluster is truncated at $n=2$, i.e., only the one- and two-point correlations are included, the corresponding cluster variation method is generally referred to as the Bethe analysis. A systematic method to derive entropy expression for a cluster containing more than two spins has also been developed. In the present work, we used the square-cluster ($n=4$) approximation, of which the entropy formula can be found in Ref. [55].

Although the nature of the cluster variation method is such that all critical exponents for continuous phase transitions are classical, reasonably accurate values for the critical temperature can be obtained with a limited computational effort. As a test, we fixed the coupling at $K=K_t$, the cluster variation method yields then the tricritical point as $D_t=3.233$, which agrees with the transfer-matrix result $D_t=3.230\,179\,7(2)$ up to the third decimal place. Since the correlations at tricriticality are long ranged while those along the first-order transition line are short ranged, we would expect that the results from the square-cluster approximation of the cluster variation method are at least reliable up to the third decimal place. The results are shown in Table VI.

V. DISCUSSION

We investigate the geometric distributions of the vacancies in the two-dimensional Blume-Capel model. At the tricritical point (K_t, D_t), critical clustering phenomena are observed for percolation clusters between vacancies, while such phenomena are absent along the critical line $D_c(K)<D_t$.

At tricriticality, the percolation clusters of vacancies and those of Ising spins of the same sign are closely analogous, as reflected by the fractal dimensions of both types of clusters. At the random-cluster fixed point $p_b=1-\exp(-2K)$, the scaling of the Ising-spin clusters is well understood because of the exact mapping between the Potts model and the random-cluster model. Such a mapping has so far not been found for percolation clusters between the vacancies. Nevertheless, it is still possible to partly explain the similarity of the Ising-spin and the vacancy clusters at tricriticality. Just as for the vacancy, the nearest-neighbor spin product $t_{ij}=s_i s_j$ is also an energylike variable. It is clear that the Ising-spin clusters are closely related to those similarly defined for the product variable t_{ij}. According to universality, clusters of different sorts of energy variables may well have the same scaling dimension.

Along the Ising critical line, however, the vacancy clusters remain finite, although the vacancy density ρ still displays critical fluctuations. At criticality, the vacancies are, just like the energy density, more or less uniformly distributed over the lattice. In order to demonstrate this point, two typical configurations of the Blume-Capel model are shown in Fig. 11 and 12 for the critical and tricritical systems, respectively.

From a comparison of our numerical results and the Kac formula (see Table II) for the tricritical Ising model, exact values of critical exponents describing critical singularities of the vacancy clusters can be obtained. These exact values can be considered as conjectures, which relate the scaling dimension of the vacancy clusters to the numbers in the Kac table.

ACKNOWLEDGMENTS

We are indebted to Dr. J. R. Heringa for valuable discussions and to X. F. Qian for deriving the transfer-matrix re-

sults for the Blume-Capel model. One of us (Y.D.) would also like thank Dr. A. J. Böttger for her knowledge about the cluster variation method. This research was supported by the Dutch FOM foundation ("Stichting voor Fundamenteel Onderzoek der Materie") which is financially supported by the NWO ("Nederlandse Organisatie voor Wetenschappelijk Onderzoek") and by the National Science Foundation of China under Grant No. 10105001.

[1] M. Blume, Phys. Rev. **141**, 517 (1966).
[2] H. W. Capel, Physica (Amsterdam) **32**, 966 (1966); Phys. Lett. **23**, 327 (1966).
[3] L. Onsager, Phys. Rev. **65**, 117 (1944).
[4] For a review, see, e.g., I. D. Lawrie and S. Sarbach, in *Phase Transitions and Critical Phenomena*, edited by C. Domb and J. L. Lebowitz (Academic Press, London, 1984), Vol. 9, p. 1.
[5] B. M. McCoy and T. T. Wu, *The Two-Dimensional Ising Model* (Harvard University Press, Cambridge, MA, 1968).
[6] R. J. Baxter, J. Phys. A **13**, L61 (1980); J. Stat. Phys. **26**, 427 (1981).
[7] D. A Huse, Phys. Rev. Lett. **49**, 1121 (1982); R. J. Baxter and P. A. Pearce, J. Phys. A **16**, 2239 (1983).
[8] B. Nienhuis, A. N. Berker, E. K. Riedel, and M. Schick, Phys. Rev. Lett. **43**, 737 (1979).
[9] B. Nienhuis, in *Phase Transitions and Critical Phenomena*, edited by C. Domb and J. L. Lebowitz (Academic Press, London, 1987), Vol. 11, p. 1.
[10] A. A. Belavin, A. M. Polyakov, and A. B. Zamolodchikov, J. Stat. Phys. **34**, 763 (1984); D. Friedan, Z. Qiu, and S. Shenker, Phys. Rev. Lett. **52**, 1575 (1984).
[11] J. L. Cardy, in *Phase Transitions and Critical Phenomena*, edited by C. Domb and J. L. Lebowitz (Academic Press, London, 1987), Vol. 11, p. 55.
[12] J. L. Cardy, Nucl. Phys. B: Field Theory Stat. Syst. **240** [FS12], 514 (1984); Nucl. Phys. B **324**, 581 (1989).
[13] L. Chim, Int. J. Mod. Phys. A **11**, 4491 (1996).
[14] I. Affleck, J. Phys. A **33**, 6473 (2000).
[15] Y. Deng and H. W. J. Blöte, Phys. Rev. E **70**, 035107(R) (2004).
[16] M. P. M. den Nijs, Phys. Rev. B **23**, 6111 (1981).
[17] H. W. J. Blöte and M. P. M. den Nijs, Phys. Rev. B **37**, 1766 (1988).
[18] There is a typo in Ref. [9] about the second magnetic exponent; from private communications with B. Nienhuis, we have $y_{h2}=9/8$ for the tricritical BC model in two dimensions.
[19] P. W. Kasteleyn and C. M. Fortuin, J. Phys. Soc. Jpn. **46** (Suppl.), 11 (1969).
[20] C. M. Fortuin and P. W. Kasteleyn, Physica (Amsterdam) **57**, 536 (1972).
[21] A. Coniglio and F. Peruggi, J. Phys. A **15**, 1873 (1982).
[22] Y. Deng, H. W. J. Blöte, and B. Nienhuis, Phys. Rev. E **69**, 026114 (2004).
[23] Y. Deng, H. W. J. Blöte, and B. Nienhuis, Phys. Rev. E **69**, 026123 (2004).
[24] Y. Deng and H. W. J. Blöte, Phys. Rev. E **70**, 046106 (2004).
[25] B. Nienhuis, J. Phys. A **15**, 199 (1982).
[26] M. E. Fisher, Physics (Long Island City, N.Y.) **3**, 25 (1967).
[27] M. F. Sykes and D. S. Gaunt, J. Phys. A **9**, 2131 (1976).
[28] A. Coniglio, C. R. Nappi, F. Peruggi, and L. Russo, J. Phys. A **10**, 205 (1977).
[29] F. Y. Wu, Rev. Mod. Phys. **54**, 235 (1982).
[30] H. Whitney, Ann. Math. **33**, 688 (1932).
[31] R. H. Swendsen and J. S. Wang, Phys. Rev. Lett. **58**, 86 (1987).
[32] U. Wolff, Phys. Rev. Lett. **62**, 361 (1989).
[33] L. Chayes and J. Machta, Physica A **254**, 477 (1998).
[34] X. F. Qian, Y. Deng, and H. W. J. Blöte, Phys. Rev. E **71**, 016709 (2005).
[35] H. W. J. Blöte, E. Luijten, and J. R. Heringa, J. Phys. A **28**, 6289 (1995).
[36] H. W. J. Blöte, L. N. Shchur, and A. L. Talapov, Int. J. Mod. Phys. C **10**, 1137 (1999).
[37] Y. Deng and H. W. J. Blöte, Phys. Rev. E **68**, 036125 (2003).
[38] J. R. Heringa and H. W. J. Blöte, Physica A **232**, 369 (1996); Phys. Rev. E **57**, 4976 (1998).
[39] D. Stauffer and A. Aharony, *Introduction to Percolation Theory* (Taylor and Francis, London, 1992), and references therein.
[40] K. Binder, Z. Phys. B: Condens. Matter **43**, 119 (1981).
[41] Y. Deng and H. W. J. Blöte, Phys. Rev. E **71**, 016117 (2005).
[42] P. D. Beale, Phys. Rev. B **33**, 1717 (1986).
[43] X. F. Qian, Y. Deng, and H. W. J. Blöte (unpublished).
[44] Y. Deng and H. W. J. Blöte, Phys. Rev. E **70**, 046111 (2004).
[45] Y. Deng, J. R. Heringa, and H. W. J. Blöte, Phys. Rev. E **71**, 036115 (2005).
[46] M. E. Fisher, Phys. Rev. **176**, 257 (1968).
[47] R. M. Ziff, Phys. Rev. Lett. **69**, 2670 (1992).
[48] M. E. J. Newman and R. M. Ziff, Phys. Rev. Lett. **85**, 4104 (2000); Phys. Rev. E **64**, 016706 (2001).
[49] G. Kamieniarz and H. W. J. Blöte, J. Phys. A **26**, 201 (1993).
[50] P. Di Francesco, H. Saleur, and J.-B. Zuber, Nucl. Phys. B: Field Theory Stat. Syst. **290** [FS20], 527 (1987).
[51] P. Di Francesco, H. Saleur, and J.-B. Zuber, Europhys. Lett. **5**, 95 (1988).
[52] J. Salas and A. D. Sokal, J. Stat. Phys. **98**, 551 (2000).
[53] R. Kikuchi, Phys. Rev. **81**, 988 (1951).
[54] D. M. Burley, in *Phase Transitions and Critical Phenomena*, edited by C. Domb and J. L. Lebowitz (Academic Press, London, 1987), Vol. 2, p 329.
[55] J. M. Sanchez and D. de Fontaine, Phys. Rev. B **17**, 2926 (1978).
[56] T. Mohri, J. M. Sanchez, and D. de Fontaine, Acta Metall. **33**, 1171 (1985).
[57] M. I. Pekelharing, A. J. Böttger, M. A. J. Somber, and E. J. Mittemeijer, Metall. Mater. Trans. A **30**, 1945 (1999).